Hurricane tritium II: Air-sea exchange of water in Betsy 1965[1]

By H. GÖTE ÖSTLUND, *Institute of Marine Sciences, University of Miami*

(Manuscript received December 12, 1967; Revised)

ABSTRACT

The radial and vertical distribution of tritium (as HTO) in rain water and in water vapor was investigated in hurricane Betsy on four days, each day having different storm characteristics. On one day, 3 September, stratospheric subsidence was detected in the eye. The tritium concentration of underlying seawater was also measured. The molecular exchange of water at the air/sea interface was clearly exhibited on all four days, and the extent of exchange increased with increasing storm intensity. On 3 September the wall cloud vapor had a composition equivalent to 86 % seawater vapor and 14 % vapor from outside the storm envelope.

Together with the measured radial distribution of total wind velocity and reasonable assumptions of the effect of spray on rate of exchange, the tritium data were used to calculate possible distributions of relative inflow angle and of specific vapor inflow. A maximum in the inflow function around 120 km was obtained in one case, indicating subsidence between 200 km and 120 km. In the same area the distribution of tritium changes drastically from a vertical gradient to vertically well mixed and a horizontal gradient.

Introduction

Virtually all of the tritium now found on earth was produced by the fusion bomb tests, particularly the 1961–1962 United States and U.S.S.R. experiments. Most of the bomb tritium was injected into the stratosphere, from where it is being transferred as tritiated water, HTO, to the troposphere. The time scale for this process is of the order of a few years (Craig & Lal, 1961; Brown *et al.*, 1961). After stratospheric water, tagged by HTO, has entered the troposphere, it is removed as rain within a relatively short period of time and is carried to the continents or the oceans. Molecular exchange of water vapor at the air-sea interface is another mechanism by which tritium is transferred to the ocean. Once tritium enters the ocean, it is rapidly distributed in the well-mixed layer above the thermocline. This layer, some 100 to 200 meters deep, contains such a large mass of water that the tritium concentration is considerably lower than that of the water vapor of the air.

The physical and chemical properties of HTO are practically identical with H_2O. The meteorological source of HTO is the stratosphere, and its sink is the ocean, at least as a first approximation. Tritium, therefore, offers a unique tool for the study of the transfer of water in nature. Some work has been done on global-scale atmospheric phenomena utilizing tritium measurements (e.g., Bolin, 1959; Eriksson, 1965), but the potential for the study of mesoscale meteorological processes is virtually untapped. In addition to hurricane problems, tritium measurements could be used to study cloud and rain formation, fair weather air-sea exchange, air-mass modifications and entrainments of various kinds. The average tritium level in atmospheric vapor is decreasing and, as this paper is being written, difficulties are appearing in the application of this method at low latitudes.

Deuterium, the other heavy hydrogen isotope, offers a valuable complement to tritium studies. In fractionation processes, deuterium water, HDO, behaves similarly to HTO, but it differs in atmospheric distribution and source-sink conditions (Friedman, 1953; Craig, 1961; Dansgaard, 1964).

[1] Contribution No. 929 from the Institute of Marine Sciences, University of Miami.

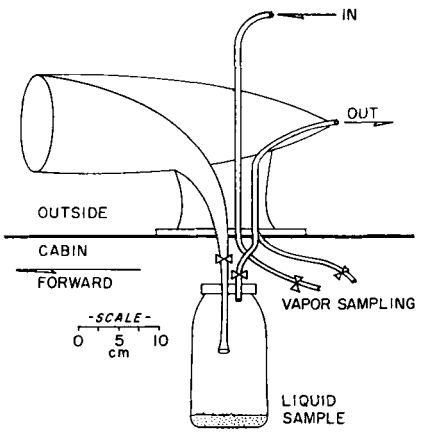

Fig. 1. Liquid water sampling system on airplane.

Statement of the Problems

Seawater, tropospheric vapor, and stratospheric vapor are characterized by different tritium concentrations. The sea surface is at the lower end of the concentration range, the tropospheric water is intermediate, and the stratospheric vapor highest. These differences in concentration allow the investigation of two phenomena in hurricanes:

1. As the undisturbed air around the hurricane, "ambient air", is entrained into the envelope of the storm, air-sea exchange will lower the tritium concentration of the water vapor. This reduction occurs through molecular exchange, including evaporation, which takes place primarily at the surface of spray droplets of seawater. The lowering of the tritium concentration in the vapor is a quantitative measure of a magnitude of air-sea exchange of water, and can be related to the mesoscale structure of the storm envelope.
2. There is a question of whether the properties of a well developed eye are to some extent due to subsidence of stratospheric air. If significant stratospheric subsidence occurs, the water vapor in the eye should have a higher tritium content than that of the inner convective area.

Experimental Procedure

Samples of liquid water and of vapor were collected on board aircraft flying through the storm. The airplanes utilized were primarily the two DC-6s operated by the Research Flight Facility of ESSA. Rainwater was also collected at ground stations. The very low specific activity of the water samples necessitated enrichment of most samples, and low-level gas counting of the weak β-activity of the tritium.

The *concentration* of tritium in water, liquid or vapor, is usually specified in tritium units (TU), which is numerically equal to the number of tritium atoms per 10^{18} normal hydrogen atoms. One TU is equivalent to a disintegration rate of 7.18 dis min^{-1} in one liter of water or an activity of 3.2 pC lit^{-1}. The *quantity* of tritium in a parcel of water is obtained by multiplying the TU figure by grams of water: One TUg is equivalent to $6.69 \cdot 10^4$ tritium atoms.

Liquid Water Sampling

A scoop with 100 cm^2 circular opening was mounted outside the fuselage. The shape of this collector, shown in Fig. 1, is such that all drops entering the scoop were swept to its narrow end, from where the water was discharged into one of two collecting bottles inside the cabin. Since the cabin was pressurized, the system was vented to the outside. The collecting bottles were standard widemouth, one liter jars; a valve arrangement allowed uninterrupted sampling, since one jar could be changed while the other was being filled.

As the air flow rate into the scoop was too low to yield isokinetic conditions at its mouth, this arrangement discriminated against very small droplets, which could easily be deflected with the air stream. However, since most of the liquid water mass in rain resides in large drops, this was not a major concern.

The scoop also collects some cloud droplets in non-raining cumulus and stratiform clouds, however, the only samples analyzed were those collected in rains which yielded sampling rates larger than 10 ml min^{-1}. No sample smaller than 20 ml was accepted, and most samples were 250–500 ml. The first few 100 ml of rain collected on each flight was assumed to be contaminated by accumulated ground-level dust and was therefore discarded. The rain water samples were transferred in the laboratory from the widemouth collecting jars to standard glass bottles with plastic seal screw caps.

Water Vapor Sampling

The desirability of collecting many (50 or more) large samples (preferably 25 g each) on

each flight, the relatively limited space in the airplane, and the frequently rough ride, ruled out direct freezeout methods utilizing liquid coolants for vapor sampling. Therefore, several solid absorbants were tested and "Molecular Sieve 4 A" was chosen. This material is a synthetic silicate having an extremely high affinity for water, indeed, the absorbed water cannot be removed entirely. The water absorbing property of this material was investigated (Östlund, 1967), and the sampling and recovery systems were designed accordingly.

Glass sample cells, called sieve traps, were made in two sizes holding 100 g and 300 g, respectively, of absorbant (see Fig. 2). Samples were collected during the flight by pumping as large an amount of air through the trap in as short a time as practical, depending on the absolute humidity of the sampled air; sampling times were in the range of 3 to 50 min.

During the1965 flights, outside air was pulled in through an aft-facing inlet tube, cf. Fig. 1, passed through the sieve trap, through a pump, and then released to the outside. The capacity of this system was about 70 l min^{-1} of air. This rate turned out to be marginal, so the airflow was increased for the 1966 season by tapping compressed air from the cabin pressurization system.

In the laboratory, the water was desorbed by gradually heating the sieve trap to 550°C while pumping through a freeze trap at −72°C, until the pressure was down to a few μb. The freeze trap containing water sample was removed and the sieve trap pumped for another ten hours at 550°C. Even after such a treatment, the sieve trap still retains 0.10 to 0.15 g of water per 100 g of absorbant (Östlund, 1967). Since 3–12 g (optimum 10 g) of water vapor per 100 g of sieve was collected in the traps on hurricane flights, the memory effect would be insignificant as long as the tritium concentration of two consecutive samples in the same sieve trap do not differ by more than a factor of two. However, in order to avoid cross-contamination from sample to sample, the following precaution was taken: After having baked the sample out of a sieve trap, 2 g of tritium-free water was absorbed per 100 g absorbant and then desorbed according to the standard procedure. The "memory water" left in the sieve trap by this procedure was low enough in tritium so as not to affect the TU value of the

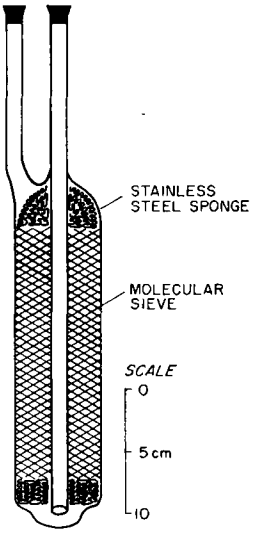

Fig. 2. Sieve trap absorption cell, for collection of water vapor. Size 300 g.

subsequent sample. This "flush" procedure, although time-consuming, was applied to every new sieve trap and to every sieve trap that had been exposed at 2000 m altitude or above, or to known high tritium content vapor. A complete record was maintained of each of the sieve traps employed in this project.

The collection efficiency of the sieves was tested by forcing moist air at 150 l min^{-1} through two 100 g sieve traps in series. In several experiments, up to 8.5 g were absorbed in the leading sieve trap, and less than 0.05 g absorbed in the second trap.

Seawater Sampling

Samples of surface and shallow depth seawater were collected by this Institute's ships during their scheduled cruises and also by privately owned small boats throughout the area. For obvious reasons, no samples were collected during storms, but samples collected before and after storm passage were deemed representative of the sea surface during the storm.

Analytical Procedure

The analytical procedure will be described elsewhere (Östlund & Rinkel, 1968), and only outlines will be given here.

In samples of sufficient size, the tritium was enriched to achieve a higher accuracy and/or a

Table 1. *Double Checks*

Flight no.	Sample no.	Sample vol., ml	Run no.	Enrichment	Result TU	Average TU
50903A	STA 319	13.4	R 479	4 ×	79 ± 3	78 ± 3
			R 488	Dir.	77 ± 7	
50903A	BOTA 1	155	R 504	10 ×	50 ± 2	50 ± 2
			R 653	40 ×	51 ± 2	
50903B	BOTB 14	550	R 472	10 ×	20.3 ± 0.8	20.1 ± 0.8
			R 686	100 ×	19.8 ± 0.8	
50903B	STB 110	8.6	R 460	3 ×	37 ± 2	38 ± 2
			R 469	Dil.	46 ± 8	
50908	Rain 10	500	R 840	100 ×	34.2 ± 1.2	
			R 1334	70 ×	34.9 ± 1.2	34.5 ± 1.1

Note: Dir. = No enrichment, direct count
Dil. = Insufficient amount, sample diluted for counting
BOT = Liquid water
ST = Vapor sample
Rain = Ground level rain

shorter counting time. The periodic addition type of electrolytic enrichment, described in detail by Östlund and Werner (1962) and by Östlund & Lundgren (1963) was used. However, the procedure has been somewhat simplified, in that the numerical values and constancy of electrolytic enrichment factors were checked by preparing samples with known tritium content and running them simultaneously with the unknown samples. Samples between 10 ml and 250 ml were reduced to 2.5 ml before counting. Every fifth run was a blank of tritium-free water which served to monitor contamination in the Laboratory. Blank values obtained were always considerably smaller than the overall error quoted in this report.

In order to measure the activity of the enriched sample by internal gas counting, the water was converted to hydrogen. For this purpose, 2.1 g of the water was reduced by magnesium metal at 570°C in a vacuum system. The counter of 1.00 liter active volume was filled to 0.34 atm (5.0 psia) with propane, after which the purified sample hydrogen was released to it until the total pressure was 2.38 atm (35.0 psia). The absorption and filling procedure was found to introduce a slight isotopic fractionation, the tritium concentration in the last hydrogen released from the charcoal being slightly higher than in the bulk gas sample. The entire procedure was standardized so that the standard deviation in isotopic fractionation was only about ±1%.

The low level counting assembly is similar to that used for the radiocarbon dating facility described by Östlund *et al.* (1962). Operating voltage for the hydrogen-propane mixture is about 4700 volts and threshold pulse height 1 mV. Typical resolution is 102.0 TU/cpm and background 1.65 ± 0.03 cpm. Tritium disintegration rates were determined to a standard deviation of ±2% or ±0.05 cpm, whichever was reached first, depending on count rate. Counting times ranged from 20 min to 20 hrs. The disintegration rates, and thereby the TU values, were corrected for the radioactive decay occurring between the times of sample collection and counting. Thus, the TU figures are valid for the date of sampling.

Overall Error and Reliability of the Tritium Measurements

The compounded standard deviation, or error, for each TU value varied according to size of sample, counting time, temporary difficulties, etc. As a rule, it was ±4% for an enriched sample and ±6 TU for a direct run (no enrichment). These errors can be considered as standard deviations (1σ), but deviations larger than 2σ should be less probable than what is predicted by the normal distribution because of contributions from non-statistical errors.

The TU values are referred to the National Bureau of Standards "Standard 4926, Tritiated Water of 20 August 1954", corrected for decay to date of use. The radioactive half life used in these calculations is 12.26 years. In order to check the reproducibility of the analytical

Table 2. *Tritium Content of Sea Surface Water 1965*

Sample locations		Date mo., day	Depth meter	Tritium conc. TU
Barbados				
In the Atlantic, 25 km SW of the island	12°50′ N, 59°45′ W	07.26	0	9.3
Antigua				
Guadelope Passage, SE of the island	16°55′ N, 61°45′ W	08.11	0	9.4
		08.26	0	8.5
		09.09	0	8.8
Puerto Rico, South				
15 km S of Paraguena Bay, in the Caribbean	17°52′ N, 67°06′ W	07.28	0	9.0
		08.25	0	9.1
		09.04	0	9.7
		09.25	0	9.5
Caicos, South Bahamas				
Turks Island Passage	21°08′ N, 71°33′ W	09.01	0	13.5
Green Turtle Cay, North Bahamas				
Atlantic side: (a) inside reef,	26°50′ N, 77°16′ W	09.09	0	15.1[a]
(b) 1 km outside reef,		09.09	0	14.0[b]
(c) 5 km outside reef		09.09	0	14.4[c]
Straits of Florida				
IMS N-1	26°21′ N, 79°23′ W	09.02	0	12.8
N-2	26°02′ N, 79°45′ W	09.02	0	11.2
H-1	25°40′ N, 80°00′ W	08.27	0	14.1
H-2	25°33′ N, 79°40′ W	08.27	0	11.6
	Same	09.24	0	9.9
	Same	09.24	10	10.1
	Same	09.24	20	10.2
H-3	25°33′ N, 79°25′ W	08.28	0	12.2
	Same	08.28	10	12.7
H-7 At edge of Florida reefs	24°50′ N, 80°31′ W	08.29	0	19.8
	Same	08.29	10	18.7
	Same	08.29	20	20.4
H-4 Shallow water	24°37′ N, 79°09′ W	08.28	0	15.1
H-6	24°30′ N, 80°30′ W	08.29	0	11.0
	Same	08.29	10	11.1
	Same	08.29	20	10.8
	Same	09.26	0	10.3
	Same	09.26	10	9.7
	Same	09.26	20	9.4
H-5	24°05′ N, 79°25′ W	08.29	0	12.8
	Same	08.29	10	12.5
	Same	08.29	20	12.1
	Average Straits of Florida Stations			12.75
	Caicos			13.5
	Green Turtle Cay Outside Reef			14.2
	Grand average Bahamian area			13.5

method, a number of samples were split and the two portions processed differently. The results obtained are listed in Table 1.

Experimental Results

Seawater Samples

The geographic locations of the sea surface samples are plotted in Fig. 3 as small squares. Table 2 gives the result of the analysis of the samples directly associated with the hurricane, and also certain other surface water stations for comparison.

The grand average of 13.5 TU includes, with equal weight, the averages for Caicos, Green Turtle Cay and the Straits of Florida only. This figure is used in all subsequent calculations, except for 29 September, when 11 TU seems

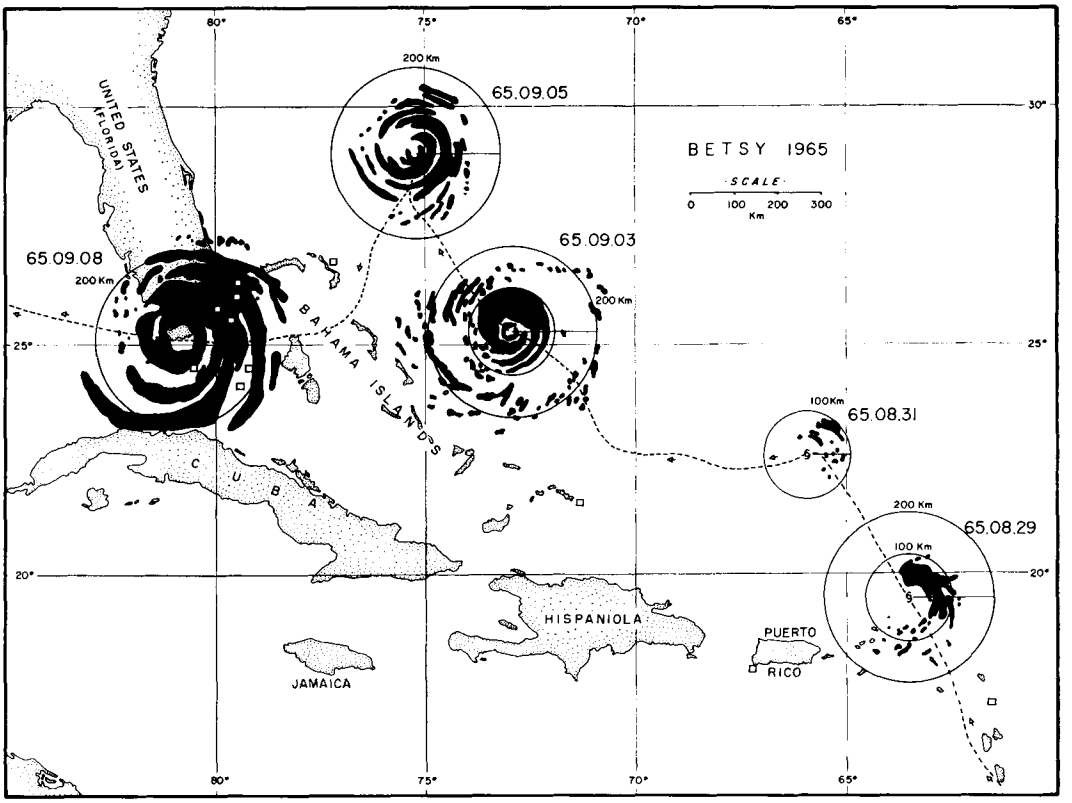

Fig. 3. Chart of track of Betsy with approximate locations and radar pictures on sampling days, 29 and 31 August, 3, 5 and 8 September. Squares are sampling locations for seawater.

more appropriate. Each station in the Straits was carried with equal weight in computing the Straits of Florida stations average. Samples H-7 and H-4 were taken on the shelf edge of the reef, the water depth over the reef being less than 20 m; these samples were included in the average to reflect the contribution of vapor from the shallow areas over which parts of Betsy's circulation passed.

Atmospheric Samples

The average positions of Betsy on the days of sampling are plotted in Fig. 3. The approximate extent and shape of the rain area, as revealed by radar, is indicated.

Most flight patterns consisted principally of circumnavigation as a 110 km radius with several diametral crossings. These flights, designated "A" and "B", were planned and flown for other projects, and the tracks were not the most suitable for the tritium investigation. Pertinent meteorological and other data, collected during each flight, were compiled and averaged for the time period of each separate sample collection. These data were: sampling time, beginning and end; sample location in virtual latitude and longitude from center, in km; bearing and radial distance from center; actual total wind and relative radial wind (relative to the storm center); radar altitude; D-value; air temperature; relative humidity, absolute humidity and water mixing ratio; sample number, analysis number; TU-value, tritium mixing ratio (TMR), in TUg/kg of air. The resulting table for 131 samples is, however, too large to be reproduced in this paper.

29 August 1965. Flight 60829 B, at 700 m altitude, was undertaken while Betsy was intensifying into a hurricane. Central pressure was 997 mb at sea level; the rain covered the NW quadrant and the E semicircle; the highest wind, 30 m sec^{-1}, was measured 60 km E of the

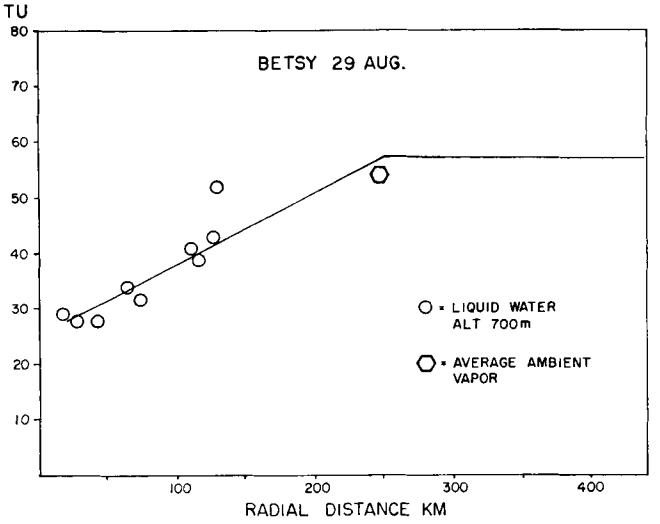

Fig. 4. Radial distribution of tritium on 29 August. Equation of line: $T = 24.87 + 0.129\ r$. The storm in formation stage.

center. Due to technical difficulties with the vapor absorption procedure, only liquid water samples were collected. In Fig. 4 are plotted the TU values versus radial distance regardless of direction from the center. In Figs. 4, 5, 6, and 7, the hexagon at 250 km indicates the average TU-value for all samples below 2500 m altitude and at a distance well outside the storm envelope on 3 and 5 September. Samples of this group are subsequently referred to as ambient samples.

31 August 1965. Flight 50831 A, at 1500 m altitude, revealed Betsy to be in a somewhat confused state, with weak banding, a poorly defined eye and highest winds of about 20 m sec^{-1}. Liquid samples were collected in all quadrants. See Fig. 5.

3 September 1965. By this time Betsy was

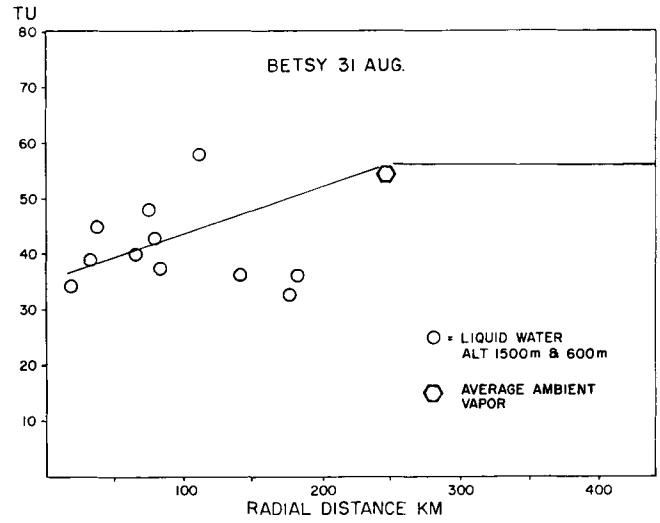

Fig. 5. Radial distribution of tritium on 31 August. Equation of line: $T = 35.30 + 0.083\ r$. The storm poorly organized.

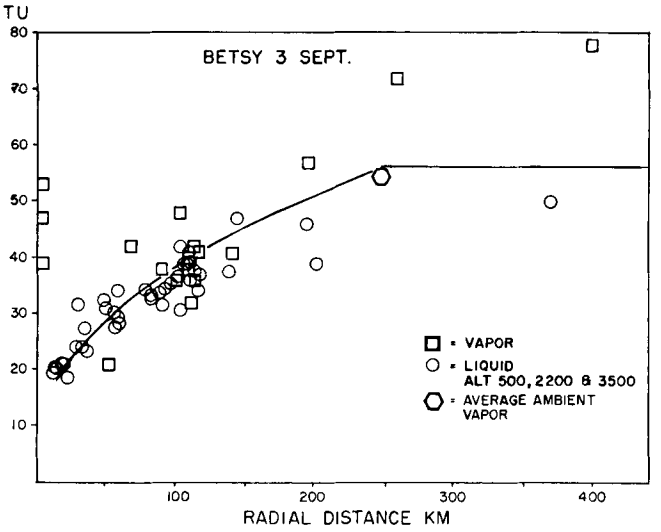

Fig. 6. Radial distribution of tritium on 3 September. Equation of curve: $T = 6.11 + 3.172\sqrt{r}$. The storm very well organized.

well organized. The storm was symmetrical, with well-developed banding to about a 200 km radius in all quadrants; it had a well-defined eye of about 30 km diameter with a lowest surface pressure of 946 mb. Part of the time there was a lower, inner circular cloudwall separated from an outer higher ring of wall clouds. Maximum winds were about 60 m sec^{-1}. Sampling of vapor and liquid was performed on two flights this day; 50903 A, mainly at 3500 m, and 50903 B, at 2200 m and 600 m. See Fig. 6.

5 September 1965. Not quite as intense as on the 3rd, Betsy now had a center surface pressure of 970 mb and maximum winds of 45 m sec^{-1}. The rain area extended to all quandrants. Sampling of both vapor and liquid was made on three flights: 50905 A at 3500 m, 5700 m

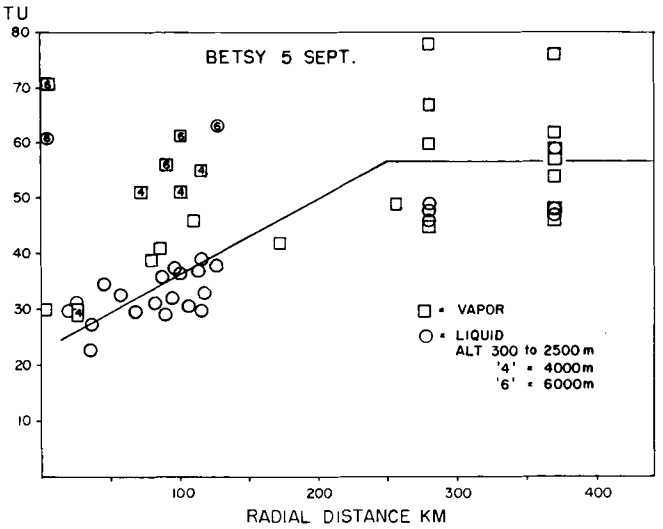

Fig. 7. Radial distribution of tritium on 5 September. Equation of line: $T = 22.80 + 0.135\ r$. The storm well organized.

Table 3. *Ground Level Rains, July–September 1965*

A. Institute of Marine Science. 25°44′ N, 80°10′ W, Altitude 15 m

Time period	Sample pos. rel. to center of Betsy dir., km	Wind direction	Amount of rainfall mm	Tritium TU
July, all rains	—	—	—	71
Aug. all rains	—	—	—	61
Aug. 3–15	—	—	45	53
Aug. 16	—	E-SE	12	57
Aug. 23–24	—	—	5	71
Aug. 30	NNW 1400	E	14	66
Sept. 7	W 270	N	8	41
Sept. 8, (24 hrs)	WNW–ENE*	—	185	27.8
Sept. 13–30	—	—	150	35.0

* Chord, shortest radial distance 65 km N of center.

B. Coral Gables. 25°42′ N, 80°16′ W, Altitude 10 m

Date mo., day	Time GMT	Sample pos. rel. to center °, km	Tritium TU
09.07	14.30	278/270	46
09.08	00.10	287/183	40
09.08	03.00	292/159	40
09.08	04.55	303/117	38
09.08	07.00	318/83	32.6
09.08	10.30	010/67	31.2
09.08	15.30	068/131	32.6
09.08	21.30	083/277	34.6

and 800 m; 50905 B at 2200 m and 700 m; 50905 E sampled vertical profiles at distances of 280 km and 350 km from the center in all quadrants, Fig. 7. The samples from the E-flight, together with a few enroute samples at >250 km distance, collected on other flights on this day and on 3 September, form the group of samples called the "ambient" samples, because they are all from outside the main storm envelope.

Ground Level Rain Sampling. While Betsy passed from E through S to SW of Miami, samples of rain water were collected on the roof of the Institute on Virginia Key and from the roof of a house in Coral Gables, on the mainland about 2 km from the shore. For comparison, the results of these samples are reported in Table 3 together with other non-hurricane rains of the season. The tritium values from these land-based samples show the same pattern as the aircraft samples for previous days. The normal, seasonal decrease of tritium concentration in rains between July and end of September, is also obvious in the table.

Discussion

Curve Fitting

The radial distribution curves shown in Figs. 4 to 7 have been drawn from equations calculated by the least square method. In the calculations the following simplifications were made:

1. Eye samples were excluded.
2. All other tritium results were given equal weight regardless of analytical accuracy and altitude range (height increment of precipitable water column represented by each sample).
3. Samples from distances greater than 250 km, all collected on 3 and 5 September, have been grouped together and assigned the radius

Table 4. *Tritium Results and Storm Character*

Date mo., day	Lowest pressure mb	Highest winds m/sec^{-1}	Average slope of T-r-function TU km^{-1}	% Seawater vapor in wall clouds
8.29	997	30	0.13	66
8.31	990	20	0.08	43
9.03	946	60	0.16	84
9.05	970	45	0.13	65

value of 250 km. The sampling points were outside the main envelope of the storm, and the group is considered to represent "ambient air" on all four days.

4. The equations have been chosen to best fit the experimental data. They do not reflect any mathematical model.
5. The equations (given in the caption of each figure) are valid from the cloudwall out to 250 km.

The samples from 29 August, Fig. 4, and 31 August, Fig. 5, are too few and the results too scattered to justify drawing anything but a straight line.

The equation for 5 September is calculated for samples from altitudes less than 3000 m only. The reason for this will be discussed later. Applying a second order equation gave such vague indications of the sign of concavity (second derivative) that here also the straight line was preferred.

Comparison with Gross Storm Characteristics

The simplest way of comparing the tritium data with related meteorological parameters is the approach used in Table 4. Here the total decrease of tritium concentration is compared with the summarized characteristics of the storm each day. The fifth column records the composition of the wall-cloud vapor as if it were a mixture of seawater vapor and vapor from outside the storm (ambient vapor). The seawater is assumed to have had a tritium concentration of 11 TU on 29 August, when the storm was far to the south, and 13.5 TU on all other days. As will be discussed later, the decrease of tritium concentration in the vapor does not reflect net evaporation from the sea surface. But already this highly simplified approach clearly shows the increase of air-sea exchange with increasing storm intensity.

Vertical Distribution of Tritium

On 3 and 5 September, samples were collected at various altitudes, giving us the opportunity to study the vertical distribution of tritium at various radial distances. Tables 5A and B were assembled subject to the following conditions:

1. The samples were grouped according to altitude and radial distance from center, regardless of bearing and length of sampling track.
2. For each group, we calculated average tritium concentration (TU) in rain and in vapor and the average tritium mixing ratio, TMR (TU × mixing ratio), as TUg/kg of air, in rain areas and in no-rain areas. The water mixing ratios were calculated from measurements of temperature and relative humidity. The latter was assumed to be 100 % in rain areas. For each vapor sampling period, humidity data were estimated from the infrared hygrometer aboard the planes. A ±5 % uncertainty in the humidity may occur here, however, this error is of very little importance in the following discussions.
3. In computing a representative TU value for each radius (last line, Fig. 5A), the tritium values were weighed according to height increment of precipitable water column, represented by altitude spacing of samples, and the uncertainty of each TU figure.

In this connection, it should be remembered that while the liquid samples represent individual showers, the vapor sampling periods were so long that each sample may or may not include passage through showers; however, most of the vapor sampling times were spent in non-raining air.

When vapor of T_V tritium units is partly condensed to water under equilibrium conditions, the tritium concentration of the liquid drops is:

$$T_L = f_T \cdot T_V \qquad (1)$$

Table 5. *Radial and Vertical Distribution of Tritium*

The radial extent of each area and the center of gravity of the samples in each area are given in the column heads. The upper, italic figures in each square are average tritium concentration as TU, and average tritium mixing ratio, TMR, as TUg/kg of air, of vapor samples in each area and altitude. The lower figures are corresponding results for samples of liquid water collected in the same area and in computing the TMR value 100 % relative humidity was assumed here. Values listed under "250 km" are composite of both days

5A. 3 September

		Radial distance in kilometers						
Alt. meters	Eye	10–25 17	26–40 32	41–60 50	61–100 80	101–118 110	119–200 165	>250 250
5700						*36/166*		
3700				*21**		*40/300*		
		20.0/258		32.5/332	35.4/315	37.8/312		
2200	*47/766*				*38/410*	*36/403*		*64/591*
		19.5/283	25.8/362	29.9/358	33.2/389	36.3/412		54/676
1700	*45/722*							
		20.7/331	27.4/392					
1200								*62/670*
								48/638
900				31.0/487				
600					*42/580*	*41/610*	*57*/918*	*53/649*
					34.4/540	39.5/659	42.4/716	46/791
300								*46.5/670*
								48/831
Representative TU-value		*20.0*	*26.5*	*31*	*35*	*38*	*43*	*54.0*

5B. 5 September

		Radial distance in kilometers						
Alt. meters	Eye	10–25 17	26–40 30	41–70 55	71–100 90	101–127 113	128–200 173	>250 250
5700	*71*/511*				*56/314*	*61/323*		
	61/439					63/353		
3700					*51/444*	*52/395*		
			29.8/361			37.5/323		
2200	*30*/408*				*41/467*	*46/534*	*42*/491*	*64/591*
			29.2/409	31.2/402	38.0/437	32.6/409		54/676
1200								*62/670*
								48/638
900			22.8/413	34.6/619	32.0/512	37.9/595		
600								*53/649*
								46/791
300								*46.5/670*
								48/831

* One small sample, $\sigma = \pm 7$ TU.

where the fractionation factor f_T is between 1.11 and 1.09 at temperatures 14°C to 30°C (Sepall & Mason, 1960). Therefore, one would expect the rain drops to have higher TU value than the vapor. That the reverse is observed at e.g. 250 km, cf. Table 5, may be due to the phenomenon that the ascending air inside the cumulus towers carries upward vapor or drops from a lower altitude, where the TU value is lower.

At a distance of 250 km or more (last column in Table 5), the TU figures increase with altitude. This is to be expected if the source of tritium is located at the top of the air column, and the sink and a supply of low-tritium vapor is at the bottom. In the columns representing air inside the envelope, i.e., radii less than 120 km, the pattern is different. On 3 September, the TU values are constant with altitude, and TMR decreases with increasing altitude.

The vertical constancy of the TU-values is not as pronounced on 5 September. On that day, it looks as if substantial influx of ambient air occurred also above 2000 m altitude, reaching at least as far as to 70 km radius. This air was gradually mixed with lower, modified air and lifted in cumulus development. On this day, we therefore excluded samples above 3000 m in the calculation of the empirical T versus r relationship in Fig. 7 and in the air-sea exchange calculations below.

Properties of the Eye

On 3 September, both the TU and the TMR values are much higher in the eye than in the wall cloud air, a case similar to that in Hilda, 1964 (Östlund, 1967). Thus, it is impossible that the vapor in the eye originates entirely from the cloud wall on this day. A possible explanation is that the air in the eye is "old", essentially unmodified, ambient air which has been "trapped" since the formation of the circulation. However, it seems more likely that the tritium values in the eye are the result of the addition of subsiding tritium-rich, lowhumidity, stratospheric air to the moist air entering from the cloud wall. The energy of 1.2 kcal, required to evaporate 2 g of liquid water from 1 kg of wall cloud air transferred into the eye, could be obtained from the adiabatic compression of 0.05 kg of stratospheric air from 200 mb and −50°C to 800 mb and +20°C. This would require a TMR of the descending air of 7000 TUg/kg, which is not unreasonable.

Air-Sea Water Exchange

We are now going to make further calculations, utilizing the experimentally determined radial distribution of the TU values. In these calculations, we are going to disregard the effect of fractionation occurring in the evaporation and condensation processes, cf. Eq. (1). This will introduce an error, the size of which depends on the actual conditions under which each process occurs. It will depend, for instance, on how large a fraction of the water condenses in a parcel of air lifted into cumulus cloud. This error will be small in comparison with those resulting from other deficiences in the model used.

We also assume that no stratospheric air can enter the inflow layer, which is sealed by the overlying outflow. This is largely in accordance with models by Fujita *et al.* (1967) and others.

The change in tritium concentration of the atmospheric vapor, the T-values, is the result of the transfer of H_2O and HTO molecules in both directions, at the air/sea interface of spray droplets and at the ocean surface. If the number of water molecules, N_d, impacting on, and captured by the seawater phase, is larger than the number of molecules, N_u, released from the same area at the same time, we have evaporation equivalent to the difference between the two figures, $N_u - N_d$. We will find that our tritium data in principle will tell us only about the upward component N_u of the flux, and nothing directly about the net evaporation.

In addition to the deductions in this and the following chapter, another line of thoughts is expressed in the Appendix. The two paths of thinking converge in Eq. (7) and Eq. (A12) respectively.

Let us now consider a cylindrically symmetrical hurricane in steady state, with an inflow layer of such a thickness that it contains h grams of precipitable water per cm². Let us also assume that the vertical gradient of tritium concentration is negligible in this layer, which was experimentally verified. We furthermore assume a constant tritium concentration S tritium units in the seawater under the hurricane.

At a radial distance r in the inflow layer, we now consider a vertical column of air containing water vapor with tritium concentration T tritium units. By moving the air parcel dr towards the center, the tritium concentration changes by dT. This is partly caused by an upward

flux of dw grams of seawater vapor per gram of atmospheric water vapor in the inflow layer, carrying with it a tritium quantity of $S \cdot dw$. Since the height of precipitable water column is assumed constant, dw grams of water also has to be transferred from the air to the seawater, carrying with it a tritium quantity of $T \cdot dw$. The change of tritium quantity in one gram of atmospheric vapor is thus

$$dT = (S - T) \cdot dw \tag{2}$$

We will now define a specific air-sea water exchange coefficient, ψ by

$$\psi = -dw/dr \tag{3}$$

and obtain from Eqs. (2) and (3)

$$\psi = \frac{dT/dr}{T - S} \tag{4}$$

The function, ψ, expresses the fraction of water vapor in the air that is exchanged with the sea per km radial displacement of air; its dimension is km^{-1}. The advantage of ψ is that it is primarily an experimental parameter that can be used to compare different areas of one hurricane, and different hurricanes, with a minimum of assumptions of other parameters.

In Table 6, values of ψ are listed. The calculations utilized from Eq. (4) combined with the empirical equations for $T(r)$ for Betsy on 3 and 5 September. On the first of those two days, computations were originally made for both the empirically smoothed $T(r)$ curve of Fig. 6 and for the representative T-values of Table 5A. The two methods gave reasonably similar results, but the large distances between the sampling points, especially outside 100 km, gave too much scatter in the results using the latter point values. Therefore, this case is not reported here. In the 5 September values, the straight line of Fig. 7 was used. The error introduced by disregarding the fractionation is such that our computations should give ψ-values 0 to about 20% too high.

The most noticeable difference between these two days is that on 3 September, ψ increases much more sharply at small radii than on 5 September. It will be shown below how this can be related to the greater variation in wind velocity on the 3rd.

Table 6. *Specific Air/Sea Water Exchange Coefficient ψ, Total Wind u, and Relative Inflow Angles γ*

[A], [B], and [C] refer to calculations using Eq. 9A, B, and C respectively. [MR] refers to values calculated from Malkus and Riehl, 1960

r km	$\psi \cdot 10^4$ km^{-1}	u m/sec	γ[A]	γ[B]	γ[C]	γ[MR]
A 3 Sept.						
250	23.48	11.0	7.698	2.777	1.001	1.000
200	29.99	13.0	5.100	2.174	0.926	1.000
150	41.29	20.0	2.408	1.579	1.035	1.000
120	52.98	26.0	1.443	1.230	1.048	1.000
100	65.21	30.5	1.000	1.000	1.000	1.000
80	85.59	36.5	0.643	0.770	0.921	0.730
60	119.10	42.0	0.398	0.548	0.754	0.460
50	149.2	45.5	0.293	0.437	0.652	0.325
40	197.8	47.0	0.214	0.323	0.508	0.180
30	289.9	41.0	0.167	0.225	0.302	0.065
25	374.3	37.5	0.142	0.174	0.214	0.002
20	522.3	34.0	0.112	0.125	0.139	
B 5 Sept.						
250	31.37	20.0	3.170	1.893	1.130	
200	37.21	21.0	2.545	1.596	1.001	
150	45.72	25.5	1.706	1.299	0.989	
120	52.99	29.5	1.273	1.121	0.986	
100	59.38	33.5	1.000	1.000	1.000	
80	67.26	38.0	0.778	0.883	1.002	
60	77.72	34.0	0.753	0.764	0.776	
50	84.25	30.0	0.787	0.705	0.631	
40	91.98	26.5	0.816	0.646	0.511	
30	101.34	22.5	0.872	0.586	0.394	
25	106.69	20.5	0.909	0.557	0.341	

Implications on the Inflow Angle

The exchange flux of seawater vapor from the sea to the air, per geographical area and time, t, is

$$A = h \cdot dw/dt \tag{5}$$

where h is in g cm^{-2}, time in sec, and dw is dimensionless, as defined earlier. We define the inflow angle β, according to Malkus & Riehl, (1960), as the angle between the tangent and the actual wind direction, positive inwards. This angle is small ($0 < \beta < 20$ degrees) so that we can approximate the total horizontal wind, u, by its tangential component. Then the radial wind component is $u \cdot \sin \beta$, and we obtain from Eq. (3)

$$\psi = dw/dt \cdot (u \sin \beta)^{-1} \tag{6}$$

Combining (5) and (6) gives us

$$A = h \cdot u \cdot \psi \cdot \sin \beta \tag{7}$$

Knowing h and β, or the radial wind component, e.g., from calculations on the basis of vertical profiles of aircraft Doppler-wind measurements, the exchange flux A could be evaluated from Eq. (7). Let us, however, consider β unknown, and h constant, and try different types of functions for A to calculate variations in β. Absolute values of β cannot be obtained this way, so we define a relative inflow angle γ at radius r by normalizing to the values found at 100 km radius:

$$\gamma = \frac{\sin\beta}{\sin\beta_{100}} = \frac{A}{A_{100}} \cdot \frac{u_{100} \cdot \psi_{100}}{u \cdot \psi} \tag{8}$$

A is a function of the total windspeed and encompasses several parameters such as the amount of spray per m² of ocean area, the drop size distribution and the turbulence in and above the spray layer. Not knowing this function, we try the following approaches for $10 < u < 50$ m sec^{-1}:

$$A = \varrho \cdot C_0 \tag{9A}$$

$$A = \varrho \cdot C_1 \cdot u \tag{9B}$$

$$A = \varrho \cdot C_2 \cdot u^2 \tag{9C}$$

In equation 9B the constant C_1, is dimensionless and the expression is related to the equation for often used for drag. In equation 9C, C_2 can be made dimensionless by using $|u| \cdot u$ instead of u^2. The dimension of C is of no practical importance in our discussions, since the constant falls out while substituting A-values from equations 9A, B, and C into equation 8.

Appropriate values of total wind were taken from averages of Doppler wind measurements during the actual flights on 3 September and 5 September. The u-values, smoothed graphically, are listed in Table 6, together with values of γ obtained by combining Eq. (8) with either of Eqs. (9A, B or C), in the columns headed γ[A], γ[B], and γ[C] respectively.

On 3 September the wind structure of Betsy was very similar to the model moderate hurricane of Malkus & Riehl (1960). Therefore, for comparison, γ values obtained from their β, are listed in Table 6A as γ[MB]. They assumed $\beta = 20$ degrees for $r > 100$ km, and a linear β versus r relationship at smaller r.

The feature of constant β in the outer part of the circulation is exhibited in case [C] in Table 6A, but for this case our γ values decrease much more slowly than assumed by Malkus & Riehl. Their decrease of β inside 100 km radius resembles the results in case [A], which requires that the exchange flux of seawater vapor be independent of the wind velocity; this, however, seems quite improbable.

Radial Distribution of Inflow

In Table 4, the composition of the wall cloud vapor was expressed as a mixture of pure ambient vapor and pure seawater vapor. This percentage does not, however, tell us how much seawater vapor is required for the entire dilution process from the edge of the storm (250 km) to the wall clouds. For this purpose we need to know the radial distribution of the water vapor inflow.

The total horizontal transport of water vapor through a cylindrical surface of radius r, in the inflow, is

$$\Gamma = 2\pi \cdot h \cdot r \cdot u \cdot \sin\beta \tag{10}$$

where, as before, h is the amount of water vapor (precipitable water) in grams per cm² geographical surface. We normalize the values of this flux at any radius, r, to the amount of water vapor entering the circulation at 250 km radius;

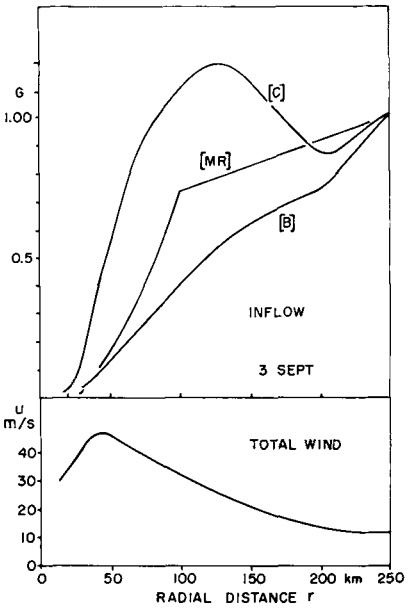

Fig. 8. Total wind (lower graph) and specific vapor inflow (upper graph) on 3 September. The inflow curves are results from use of spray functions 9B and C respectively and of β from Malkus and Riehl.

this value is referred to as the "specific vapor inflow", G

$$G = \frac{\Gamma}{\Gamma_{250}} = \frac{r \cdot u \cdot \sin\beta}{250 \cdot u_{250} \cdot \sin\beta_{250}} \qquad (11)$$

or, combined with Eq. (8),

$$G = \frac{r \cdot u \cdot \gamma}{250 \cdot u_{250} \cdot \gamma_{250}} \qquad (12)$$

and we use the values γ and u of Table 6 to compute $G(r)$. If we also assume a constant average water mixing ratio in the inflow layer, G will express the specific air mass inflow.

In Figs. 8 and 9, $G(r)$ is plotted for 3 September and 5 September respectively. Here the exchange flux A is derived from Eqs. (9B) and (9C) respectively. In addition, G for 3 September has been computed and plotted utilizing β-values from Malkus & Riehl, (1960), case [MR]. The curves for smoothed total wind versus radial distance, $u(r)$, are also included for comparison.

In Case [C] for 3 September, we obtain indications of subsidence between 200 and 120 km; however, in this region we have no vertical tritium profile and thus we cannot judge if subsidence is truly occurring. It is, however, interesting to note that e.g. Fujita *et al.* (1967) has discussed subsidence in this area, and that Miller (1960) has found indications that the drag coefficient increases with the wind speed, i.e. somewhat in analogy with Eq. 9C.

Total Exchange of Seawater Vapor

We now want to attempt to compute the integral air/sea exchange of water vapor occurring within the system, while 1 g of ambient vapor is entering the circulation at 250 km radius. This quantity is easiest expressed as

$$F = \int_{r_1}^{r_2} G \cdot \psi \cdot dr \qquad (13)$$

where the vapor is moved from r_1 to r_2 km radial distance. If we should have access to values of $G(r)$, the vapor inflow, measured independently of the tritium, we would obtain unambiguous values of F from Eq. 13. Not having that, we try a few other means.

As a first approach computing F, let us assume that no air leaves the system until the air reaches the wall clouds. This is to say that Γ is constant from 250 km to any smaller radius, and $G = 1$. From Eq. (13) and Eq. (4) we obtain

$$F = \ln \frac{T_0 - S}{T_c - S} \qquad (14)$$

Here T_0 and T_c are the TU-values of vapor at the beginning and the end of the trajectory, and S the TU value of seawater. The numerical results from these computations are recorded in Table 7, "G = Constant".

In analogy with the computations of the inflow as depicted in Fig. 9, the G-values for 3 September obtained according to the assumptions of Malkus & Riehl (1960) were inserted in Eq. (13), together with the experimental ψ-values and the equation was integrated graphically. Results recorded in Table 7, "G from Malkus and Riehl".

Graphical integration of Eq. (13), based on ψ-values from Table 6, and G-values computed for Figs. 9 and 10, yielded values of F also reported in Table 7. Here we have to remember that we are working with interdependent pairs of G and ψ values, thus we will find that F is

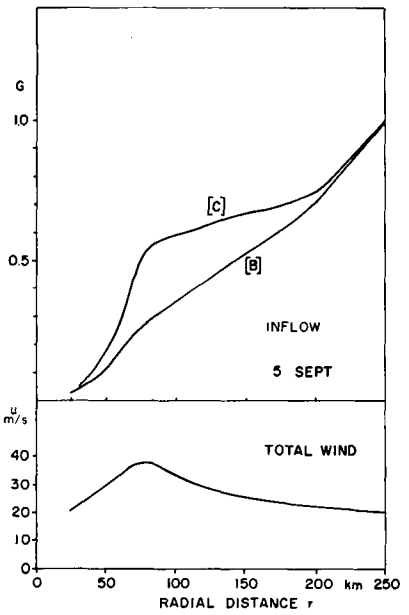

Fig. 9. Total wind (lower graph) and specific vapor inflow (upper graph) on 5 September. The inflow curves are results from use of spray functions 9B and C respectively.

Table 7. *Integrated Total Water Exchange*

For each gram of vapor in a parcel of air passing through a cylindrical surface of radius r_1 km in the inflow layer, the following quantities of seawater are transferred by exchange to the air during its transit to radius r_2 km. Cloud wall radius, cldw, was 20 km on 3 September and 25 km on 5 September

Conditions for inflow	r_1–r_2 250→100	r_1–r_2 100→cldw	r_1–r_2 250→cldw
3 September			
G = constant	0.56	1.28	1.84
G from Malkus and Riehl	0.48	0.31	0.71
G based on Eq. 9B	0.37	0.39	0.52
G based on Eq. 9C	0.60	0.50	1.16
5 September			
G = constant	0.63	0.60	1.23
G based on Eq. 9B	0.38	0.28	0.48
G based on Eq. 9C	0.46	0.30	0.63

linked to the $T(r)$-curve at one radius only, namely r_1 or 250 km. This is revealed by combining with Eq. (13) a few of the previous equations, or by direct deduction from Eq. (5); one arrives at

$$F = \frac{\psi_{250}}{250 \cdot A_{250}} \cdot \int_{250}^{r} r \cdot A \cdot dr \qquad (15)$$

which actually is not very attractive from the point of view of proper use of tritium data, since A is to be calculated from Eq. (9A, B or C).

At this point it is not possible to judge which one of the combinations in Table 7 is closest to correct. It is, however, of less practical importance. It would be more interesting to attempt to link the experimental ψ to vaguely known exchange coefficients of latent and sensible heat and of momentum, and to link F to the net evaporation. Anyway, the absolute maximum of evaporation is in the case "G = const.", where, on 3 September, the upward flux of water including evaporation is 1.84 g of seawater per g of entrained ambient vapor at 250 km radius. No minimum value of evaporation can be deducted from our data.

Implications on the Energy Budget

In the energy budget of the hurricane, the important feature is the net evaporation, not the upward exchange flux of water molecules reflected in the tritium values. If we want to estimate the net evaporation as a fraction of the total exchange, we need to consider the relative humidity of the friction layer. We also need to know if evaporation of droplets to dryness, or near dryness, is an important part of the process.

Under "equilibrium" conditions, 90% relative humidity, and evaporation mainly from the sea surface and large drops, the net evaporation should be only 1/10 of the total exchange. This can be derived in several ways, cf. for instance Ehhalt and Knott (1965). Except cases "G = Const." in Table 7, net specific evaporation would then be 0.1 g/g or less.

Let us postulate that air, lifted in the rain bands, leaves the system at any radius to the outflow, no recycling taking place. If we still assume 90% relative humidity, this *per se* limits the maximum possible addition of water to the air by evaporation, to less than 0.1 g per g of ambient vapor entrained at the edge of the storm envelope. Under these conditions the tritium data supply no new information and our discussion on the energy budget is almost trivial.

As can be observed in Table 5, particularly for 3 September, the vertical distribution of tritium changes drastically from outside to inside the storm envelope. Outside, the TU-values increase with increasing altitude, but inside they are independent of the altitude. This is true for both falling rain and the air between showers, and it is not easy to understand how this can be the result of upward transport only. It is tempting to suggest that vertical mixing takes place with ascent in the cumulus towers and local subsidence between rainbands or individual towers. In this connection it is also interesting to remember that in Fig. 8 case [C] indicated strong subsidence between 200 km and 120 km from the center. Subsidence will require addition of water to maintain the high humidity figures at the lowest altitudes. Thus recycling of the air would mean that net evaporation would be a significant part of the energy budget. The tritium data prove that the exchange is intensive enough to allow very substantial evaporation but they do not measure the evaporation.

Acknowledgements

The cooperation of the directors and staffs of ESSA, National Hurricane Laboratory and

ESSA Research Flight Facility is greatly appreciated.

The project was supported by the Atmospheric Sciences Section, National Science Foundation, under grants numbers NSF GP-4534, NSF GA-0415, and also by grant number WBG-85 from Project Stormfury, Environmental Science Services Administration.

For valuable discussions while writing this paper, I am indebted to Dr. Russell Snyder of this Institute and Dr. Hilding Sundqvist at International Meteorological Institute of the University of Stockholm.

APPENDIX

Another deduction to obtain Eq. 7

Notations:

- ϱ = density of air
- q = mixing ratio of water in air
- q_w = mixing ratio at saturation
- t = time
- T = tritium concentration of the atmospheric water vapor in TU.
- S = TU-value of seawater
- r = radial distance from storm center
- z = altitude
- v = radial component of the wind
- H = thickness of subcloud layer
- σ = vertical flux of tritium
- f = vertical flux of water vapor
- A = air/sea exchange coefficient for water

We assume axial symmetry and vertical homogeneity and derive for the changes of water and tritium in a volume element of the subcloud layer:

$$\frac{dq}{dt} = \frac{1}{\varrho}\cdot\frac{\partial f}{\partial z} = \frac{\partial q}{\partial t} + v\cdot\frac{\partial q}{\partial r} \qquad (A\,1)$$

$$\frac{d(qT)}{dt} = \frac{1}{\varrho}\cdot\frac{\partial \sigma}{\partial z} = \frac{\partial (qT)}{\partial t} + v\cdot\frac{\partial (qT)}{\partial r} \qquad (A\,2)$$

When integrating these two equations, we assume the subcloud layer to be well mixed vertically, and obtain

$$\frac{1}{\varrho}(f_H - f_0) = H\left(\frac{\partial q}{\partial t} + v\cdot\frac{\partial q}{\partial r}\right) \qquad (A\,3)$$

$$\frac{1}{\varrho}(\sigma_H - \sigma_0) = H\left(\frac{\partial (qT)}{\partial t} + v\frac{\partial (qT)}{\partial r}\right) \qquad (A\,4)$$

In a conventional way we denote the vertical fluxes at the air/sea interface as

$$f_0 = A(q_w - q) \qquad (A\,5)$$

$$\sigma_0 = A(Sq_w - Tq) \qquad (A\,6)$$

The vertical fluxes of water and tritium at altitude H can be written

$$f_H = -\varrho\cdot K\partial q/\partial z \qquad (A\,7)$$

$$\sigma_H = -\varrho\cdot K\partial (qT)/\partial z \qquad (A\,8)$$

where K is a proportionality constant.

The experimental results of the vertical constancy of the T-values in the inflow layer might allow us to consider $\partial T/\partial z = 0$ also in the subcloud layer. Also utilizing an assumption of steady state we can combine the above equations to

$$A = \varrho\cdot H\cdot\frac{q}{q_w}\cdot v\cdot\frac{\partial T/\partial r}{T - S} \qquad (A\,9)$$

The air/sea exchange ceofficient A, expresses the number of water molecules, as mass of water, that is leaving the seawater phase per unit area and time. It should be noted that A is not the net evaporation, of H_2O and HTO which is expressed by Eqs. (A 5) and (A 6). From our experimental data we calculate

$$\psi = \frac{dT/dr}{T - S} \qquad (A\,10)$$

which we insert in (A 9), together with

$$v = u\sin\beta \qquad (A\,11)$$

We obtain

$$A = \varrho\cdot H\cdot(q/q_w)\cdot u\cdot\psi\sin\beta \qquad (A\,12)$$

an equation which for all our practical purposes is equivalent to Eq. 7.

REFERENCES

Bolin, B. 1959. On the use of tritium as a tracer for water in nature. *Second U.N. Int. Conf. on the Peaceful Uses of Atomic Energy, 18*, 336–343.

Brown, F., Goldsmith, P. L., Green, H. F., Holts, A. & Parham, A. G. 1961. Measurements of the water vapor, tritium and carbon-14 content of the middle stratosphere over Southern England. *Tellus 13*, 407–416.

Craig, H. 1961. Isotopic variations in meteoric waters. *Science 133*, 1702–1703.

Craig, & Lal, D. 1961. The production rate of natural tritium. *Tellus 13*, 85–105.

Dansgaard, W. 1964. Stable isotopes in precipitation. *Tellus 16*, 436–468.

Ehhalt, D. & Knott, K. 1965. Kinetische Isotopentrennung bei der Verdampfung von Wasser. *Tellus 17*, 118–130.

Eriksson, E. 1965. An account of the major pulses of tritium and their effects in the atmosphere. *Tellus 17*, 118–130.

Friedman, I. 1953. Deuterium content of natural water and other substances. *Geochim. Cosmochim. Acta 4*, 89–103.

Fujita, T., Izawa, T., Watanabe, K. & Imai, I. 1967. A model of Typhoons Accompanied by Inner and Outer Rainbands. *Journal of Applied Meteorology 6*, No. 1, 3–19.

Malkus, J. S. & Riehl, H., 1960. On the dynamics and energy transformations in steady-state hurricanes. *Tellus 12*, 1–20.

Miller, B. I. 1960, A Study of the Filling of Hurricane Donna (1960) Over Land. *Monthly Weather Review 92*, No. 9, 389–406.

Sepall, O. & Mason, S. G. 1960. Vapor/liquid partition of tritium in tritiated water. *Can. J. Chem. Vol. 39*, 2024–2025.

Östlund, H. G. 1967. Hurricane Tritium I: Preliminary results on Hilda 1964 and Betsy 1965. *Amer. Geophys. Union, Monograph 11*, 58–60.

Östlund, H. G., Bowman, A. L. & Rusnak, G. A. 1962. Miami natural radiocarbon measurements I. *Radiocarbon, 4*, 51–56.

Östlund, H. G. & Lundgren, L. 1964. Stockholm natural tritium measurements I. *Tellus 16*, 118–130.

Östlund, H. G. & Rinkel, M. 1967. Study of advective and convective processes in the Atlantic equatorial current system by use of natural tritium. Technical Report, September 19, 1967. Institute of Marine Sciences, University of Miami.

Östlund, H. G. & Werner, E. 1962. The electrolytic enrichment of tritium and deuterium for natural tritium measurements. Tritium in the Physical and Biological Sciences, I, International Atomic Energy Agency, Vienna, 95–194.

ТРИТИЙ В УРАГАНАХ. II. ОБМЕН ВЛАГОЙ МЕЖДУ ОКЕАНОМ И АТМОСФЕРОЙ В УРАГАНЕ «БЕТСИ» 1965 г.

Радиальные и вертикальные распределения трития в дождевых каплях и водяных парах было исследовано в урагане Бетси в течении четырех дней, при чем каждый день имел различные штормовые характеристики. В первый день, 3 сентября, опускание стратосферного воздуха было обнаружено в глазе урагана; была также измерена концентрация трития в подстилающей водной поверхности. Молекулярный влагообмен на границе океан–атмосфера был ярко выражен в течении всех четырех дней и степень обмена возрастала с возрастанием штормовой интенсивности. 3 сентября водяной пар облачной стены содержал 86% паров от морской воды и 14% паров из окружающей ураган атмосферы. Используя измеренное радиальное распределение вектора скорости ветра и разумные предположения относительно влияния водяных капель на скорость обмена, данные о тритии были использованы для расчета возможного распределения угла относительного притока и удельного притока водяных паров. В одном случае максимальное значение притока было получено на радиусе в 120 км, что указывает на последующее опускание воздуха между 200 км и 120 км. В той же самой области распределение трития резко меняется от распределения с вертикальным градиентом к распределению, характеризующемуся хорошо выраженным вертикальным перемешиванием и с горизонтальным градиентом.